Journal homepage: http://gwse.iheg.org.cn

Research Article

The effect of beach slope variation on saltwater intrusion dynamics in the unconfined coastal aquifer (experimental and numerical)

Mohsen Azizi[1], Mohammad Hosein Najafimood[1], Abolfazl Akbarpour[2*], Abbas Ali Rezapour[3]

[1] *Department of Water Engineering, Faculty of Agriculture, University of Birjand, Birjand, Iran.*
[2] *Department of Civil Engineering, University of Birjand, Birjand, Iran.*
[3] *Department of Civil Engineering, Birjand University of Technology, Birjand, Iran.*

Abstract: Over-exploitation of groundwater resources often causes seawater to intrude into coastal aquifers. This study aims to evaluate how different beach slopes (90°, 75°, 60°, and 45°) affect the extent and behavior of seawater intrusion in unconfined coastal aquifers under transient conditions. A three-dimensional laboratory model was constructed to simulate seawater intrusion under varying beach slopes. Experimental data were analyzed using image processing techniques, and results were validated using the SEAWAT numerical model. Key parameters—including wedge toe length, height, and area—were measured over time to assess the transient response of the saltwater wedge. The results showed that under static conditions, flatter slopes produced larger saltwater wedges. During transient conditions following a groundwater-level decline, the wedge toe advanced approximately 57% further in the vertical slope than in the 45° slope, while the final wedge size remained smaller on the steeper beach. The wedge height stabilized earlier than the toe length and area during intrusion, whereas in the recession stage, all three indices reached equilibrium almost simultaneously. The geometry of the beach slope has a significant effect on both the extent and temporal behavior of seawater intrusion. The toe length index showed a strong relationship with wedge area and can serve as a reliable indicator of intrusion volume under both steady and transient conditions. These findings emphasize the importance of considering beach slope in the design and management of coastal aquifer systems. Understanding how slope geometry influences the evolution of the saltwater wedge can improve the prediction and control of seawater intrusion in response to groundwater-level fluctuations.

Keywords: Seawater; Image processing; Laboratory model; SEAWAT; Saltwater wedge

Received: 14 Nov 2024/ Accepted: 19 Dec 2025/ Published: 30 Apr 2026

Introduction

The phenomenon of saltwater intrusion is a natural process that has led to the pollution of many coastal aquifers worldwide (Abdoulhalik et al. 2022; Cheng et al. 2026). Typically, density differences between saltwater and the freshwater of the adjacent aquifer produce a sloping freshwater–saltwater interface, which causes saltwater to move below the level of freshwater. Pollution of water production wells and destruction of fresh groundwater resources are the essential destructive consequences of saltwater intrusion. Due to climate change and the intensification of climate change impacts, the phenomenon of saltwater intrusion is expected to progress worldwide. Therefore, it is essential to investigate the process of saltwater intrusion within water resource management (Werner et al. 2013). Rising sea levels, combined with land subsidence, pose serious risks to coastal freshwater resources. For instance, studies in Tian-

*Corresponding author: Abolfazl Akbarpour, *E-mail address*: akbarpour@birjand.ac.ir

DOI: 10.26599/JGSE.2026.9280077

Azizi M, Najafimood MH, Akbarpour A, et al. 2026. The effect of beach slope variation on saltwater intrusion dynamics in the unconfined coastal aquifer (experimental and numerical). Journal of Groundwater Science and Engineering, 14(2): 165-187.

jin and Hebei indicate that even moderate sea-level rise scenarios may result in extensive coastal flooding, highlighting the urgent need to consider sea-level rise, subsidence, and storm impacts in coastal water resource management to protect freshwater supplies and prevent seawater intrusion (Wang et al. 2019). Due to the importance of the subject, in the past decades, experimental and numerical models of saltwater intrusion have been the focus of researchers. At the same time, many numerical simulation models, such as FEMWATER, FEFLOW (Liu et al. 2012; Dalai et al. 2020; Fang et al. 2021; Dalai and Dhar, 2023), SUTRA (Goswami and Clement, 2007; Rezapour et al. 2018; Shen et al. 2020; Voss and Provost, 2010), and SEAWAT (Guo and Bennett, 1998; Abd-Elhamid and Javadi, 2011; Lyu et al. 2021; Wang et al. 2022; Abdoulhalik et al. 2022), have been used to simulate the process of saltwater intrusion in coastal aquifers (Li et al. 2018).

The SEAWAT model, as one of the advanced groundwater modeling tools, has several advantages that have been mentioned in many scientific articles. This model has a high ability to accurately simulate variable density flow, which is vital for investigating phenomena such as the mixing of salt and freshwater and the advance of saltwater in coastal aquifers; a capability that does not exist in simpler models such as MODFLOW. Also, by utilizing the structure of MODFLOW and MT3DMS, SEAWAT provides users with a simpler setup and better interpretation of results and models flow and transport in a fully coupled manner. The ability to perform complex three-dimensional simulations, numerical stability over long time periods, the possibility of defining time-varying boundary conditions (such as sea level fluctuations or pumping), as well as being free and having access to the source code, are other key advantages of SEAWAT that have made this model widely used in hydrogeological research.

Generally, the one-dimensional experiments of Schotting et al. (1999), Watson et al. (2002), Flowers and Hunt (2007) and the two-dimensional experiments of Zhang et al. (2002), Goswami and Clement (2007), Kenz et al. (2008), Rezapour et al. (2018), Shen et al. (2020), Dalai et al. (2020), Dalai and Dhar (2023), Narayanan and Eldho (2025), and Zhao et al. (2025) and three-dimensional experiments by Shen et al. (2020), Fang et al. (2021), Yang et al. (2024), Sharma and Chakma (2024), Ye et al. (2025), and Nam et al. (2025) have been conducted to investigate the process saltwater intrusion in porous media. Narayanan and Eldho (2025) investigated Saline GroundWater (SGW) pumping as a solution to reduce aquifer salinity and water intrusion in a layered aquifer with decreasing permeability with depth, both experimentally and in the field. In a study using a two-dimensional numerical model, the effect of temperature changes and geological layering on the intrusion pattern of saltwater and the performance of coastal cutoff walls was investigated by Zhao et al. (2025). Yang et al. (2024) investigated the method of injecting compressed air as an effective way to reduce saltwater intrusion in confined coastal aquifers using a three-dimensional numerical and laboratory (sand tank) model. Ye et al. (2025) studied the phenomenon of saltwater intrusion in estuarine aquifers through tidal river-groundwater interactions using a three-dimensional laboratory model. Nam et al. (2025) used a three-dimensional laboratory model (sand tank) to investigate the interaction between freshwater and saltwater under the influence of tides and freshwater injection.

To investigate the phenomenon of seawater intrusion, implementing boundary conditions on the seaside is of particular importance. Until now, most of the experimental and numerical studies conducted regarding the intrusion of seawater, such as research by Abarca et al. (2007), Liu et al. (2012), Ataie-Ashtiani et al. (2013), Mazi et al. (2013), Lu et al. (2016), Walther et al. (2017), Shen et al. (2020), Dalai et al. (2020), Abd-Elhamid and Sherif (2020), Fang et al. (2021), Lyu et al. (2021), Wang et al. (2022), Deng et al. (2022), Abd-Elaty and Polemio (2023), Gao et al. (2023), Dalai and Dhar (2023), Sharma and Chakma (2024), Yu et al. (2024) and Cao et al. (2024) have considered the beach boundary as vertical or a combination of vertical and sloping, while the intrusion of saltwater from a non-vertical beach into coastal aquifers is a common phenomenon.

The first studies regarding the influence of the slope of the aquifer bed on the intrusion of seawater were carried out by Abarca et al. (2007) using the SUTRA model. The results showed that the toe of the saltwater wedge was not sensitive to gentle bed slopes; however, with a significant increase in the slope, the toe of the saltwater wedge retreated. Liu et al. (2012) investigated the effects of seawater tides and changes in coastal slope on seawater intrusion using the FEFLOW numerical model; the results showed that the effects of tides on a milder beach are much greater than on a vertical beach and the impact of beach slope on the rate of saltwater intrusion can be expressed by a logarithmic function.

Ataie-Ashtiani et al. (2013) investigated the importance of considering the slope of the beach in the amount of seawater advancing into the aquifer and concluded that the parameter of the beach slope and the amount of saltwater that will come on the beach as a result of the increase in the seawater level are the controlling factor governing the position of the saltwater wedge in unconfined coastal aquifers. Mazi et al. (2013) also investigated the effect of sea level rise on the rate of saltwater advance in the unconfined aquifer with different bed slopes. The results showed that the relationship between saltwater advance increase and seawater level rise is non-linear and its rate depends on aquifer depth, the rate of seawater-level rise, and the freshwater inflow rate. After that, Lu et al. (2016) presented an analytical solution for seawater advance in unconfined and confined coastal aquifers with respect to bed slope based on the Dupuit-Forchheimer hypothesis and showed that for a constant flux at the land boundary, the position of the toe of the saltwater wedge depends on the bed geometry and slope.

Walther et al. (2017) examined the influence of sea slope on the behavior of seawater intrusion in coastal aquifers by employing the OPENGEOSYS open-source numerical framework, whose general features and computational structure are described by Kolditz et al. (2016). The results showed that the increase in the boundary slope on the sea side leads to a decrease in the extent of saltwater intrusion, and there is a significant relationship between the duration of saltwater intrusion and the slope of the sea beach. Shen et al. (2020), by building a 3D laboratory model and a SUTRA numerical model concluded that tides move the saltwater wedge seaward compared to the case in non-tidal conditions. Therefore, under tidal conditions, the effect of the cutoff wall on saltwater penetration is no longer evident. Dalai et al. (2020) investigated the dynamics of saltwater intrusion on a steep sandy beach with a two-dimensional laboratory model. The parameters of the saltwater wedge advance process were obtained through pore-water pressure measurement and image analysis techniques. Validations were performed with numerical simulations (FEFLOW).

Abd-Elhamid and Sherif (2020) used SEAWAT simulations to study the effect of seaside and aquifer-bed slopes on seawater intrusion. Their results showed that steeper seaside or bed slopes significantly increase intrusion length, highlighting the sensitivity of coastal aquifers to shoreline geometry. Fang et al. (2021) studied the effect of tides and tidal fluctuations on the effectiveness of subsurface dams to prevent the intrusion of saltwater and pollution of the upstream groundwater table using a three-dimensional laboratory model and the FEFLOW numerical model. Lyu et al. (2021) used the SEAWAT numerical simulation model in a study aimed at evaluating the effectiveness of management strategies, including the use of recharge wells and physical barriers, in preventing seawater intrusion into coastal aquifers. Numerical modeling approaches, including VFT3D and SEAWAT, have been extensively used to simulate seawater intrusion processes, evaluate their impacts on groundwater systems, and investigate geochemical influences on the migration of the saltwater wedge under variable-density conditions (Wang et al. 2022).

Complementary laboratory evidence by Deng et al. (2022) showed that changes in beach slope strongly influence swash hydrodynamics, which can affect the inland progression of saline water. Abd-Elaty and Polemio (2023), investigated saltwater intrusion in the Gaza aquifer coastal area with different bed slopes using the SEAWAT numerical model. The results showed that landward-sloping aquifer beds exhibit greater saltwater intrusion than seaward-sloping and horizontal beds. Cut-off walls and check dams are effective to manage saltwater intrusion in horizontal aquifer beds more than in other slopes. Gao et al. (2023) investigated the combined effect of subsurface dams and a typical stratified aquifer (two high-permeability layers with a low-permeability layer between them) on groundwater flow and salinity distribution in a tidally influenced coastal unconfined aquifer. The results provided a comprehensive understanding of the complex hydrodynamics of saltwater intrusion.

By building a two-dimensional laboratory model, Dalai and Dhar (2023) investigated the effect of changing the beach slope on the dynamics of saltwater intrusion under tidal boundary conditions. The beach in the laboratory model consisted of two vertical and inclined sections. By creating slopes of 15°, 20°, 25° and 30° in the sloping part of the beach, The experimental results showed that in the case of a steeper beach, saltwater penetration is less. Also, the time to reach stable conditions is longer in steeper slopes than in smoother slopes. The experimental results were validated using FEFLOW two-dimensional finite element numerical model. Tidal fluctuations change the hydraulic gradient across the beach slope, and this change in gradient causes a clockwise flow of saltwater in the porous medium in the intertidal zone.

Yu et al. (2024) found that artificial modifications of coastal morphology via beach nourishment could lead to notable changes in intrusion patterns, especially in heterogeneous aquifers. Cao et al. (2024) employed combined sandbox experiments and SEAWAT simulations and demonstrated that variations in beach gradient and sea-level conditions significantly modify the geometry and evolution of the saltwater wedge, reinforcing the importance of slope-related controls. Sharma and Chakma (2024), using a three-dimensional laboratory model under conditions where the contact surface of the sea and the aquifer is sloped, investigated the performance of a subsurface barrier in preventing the intrusion of seawater into layered groundwater aquifers with different permeabilities. They concluded that the height of seawater intrusion after installing the subsurface barrier decreases sequentially in different layers, and in aquifers with increasing permeability, the subsurface barrier significantly reduces seawater intrusion.

Liu et al. (2012) and Walther et al. (2017) utilized numerical modeling, while Dalai et al. (2020) and Dalai and Dhar (2023) employed a two-dimensional laboratory model, to explore how coastal slope influences seawater intrusion. Nevertheless, there has yet to be a thorough investigation into how variations in coastal slope affect seawater intrusion through the use of a combination of three-dimensional laboratory modeling, three-dimensional numerical modeling, and image processing methods.

This research presents a novel investigation into the effects of beach slope geometry on seawater intrusion using a fully three-dimensional laboratory model with a continuously sloping seashore boundary. Unlike previous studies—such as those by Liu et al. (2012), Walther et al. (2017), Dalai et al. (2020), and Dalai and Dhar (2023)—which primarily focused on steady-state conditions or simplified geometries, this study systematically explores both steady and transient conditions across a range of beach slopes (45°, 60°, 75°, and 90°).

The main innovation lies in the dynamic analysis of saltwater wedge behavior through high-resolution image processing, combined with numerical simulation using the SEAWAT code to validate the laboratory results. By introducing time-dependent monitoring of key indicators (toe length, height, and area of the wedge), the study provides a deeper understanding of the impact of slope on both the advancement and retreat of the saltwater wedge. This integrated experimental-numerical approach under varying slope conditions has not been previously reported and offers practical insights into the role of shoreline geometry in coastal aquifer vulnerability assessments.

1 Methodology

The methodology can be divided into four parts: 1) laboratory model, 2) experiment process, 3) image processing, and 4) numerical simulation. The schematic representation of the overall methodology is shown in Fig. 1.

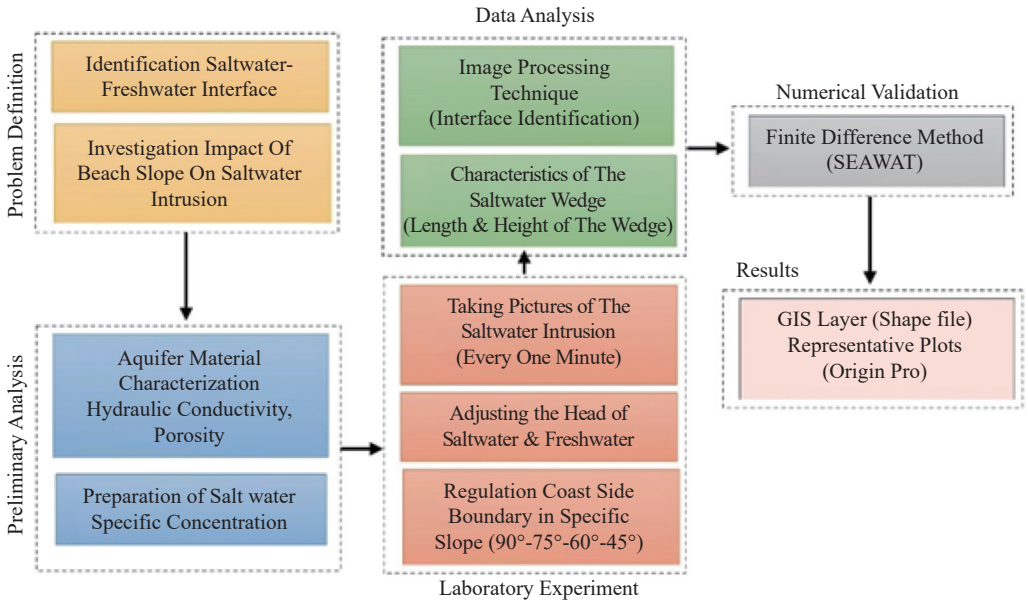

Fig. 1 Schematic representation of the overall methodology

1.1 Laboratory model

Fig. 2 shows a schematic image of the laboratory model of this research. In this study, the laboratory model of a three-dimensional flow tank with dimensions of 140 cm in length, 65 cm in height, and 40 cm in width was constructed. The flow tank was divided into three separate compartments, including a central compartment of 110 cm in length containing the porous medium (Zone B) and two side compartments of 15 cm in length on the right side to adjust the saltwater head (Zone C) and on the left side for setting the freshwater head (Zone A) and creating boundary conditions during the experiments. The front and back panels of this tank were made of transparent glass with a thickness of 10 mm to allow for image acquisition. Also, the side walls of this tank were made of galvanized metal sheets with a thickness of 5 mm.

In each of the side compartments, a 0.75-inch galvanized pipe was installed to supply the saltwater and freshwater into the side compartments of the laboratory model. Also, to adjust the saltwater and freshwater level in the side compartments (excess saltwater and freshwater overflow), a 0.75-inch galvanized outlet pipe was installed at the bottom of the side compartments. Another pipe was connected to the outlet pipes to adjust the saltwater and freshwater head for the saltwater intrusion experiments. In addition, a metal frame held the entire tank to strengthen the flow tank and support the weight of the saturated porous medium during the experiments.

Metal mesh plates (8 mm thick) separated the porous medium from the two side compartments. To prevent the particles of the porous medium from entering the side compartments, the mesh plates were covered (2 mm opening) with a fine mesh. Considering that the purpose of this research was to investigate the effect of the slope of the beach on the saltwater intrusion, the metal mesh plates on the saltwater side (right side of the laboratory model) were connected to the bottom of the tank by a hinge to allow adjustment of the beach slope angle (α). Glass beads with a diameter of 1,000 to 1,200 microns and a specific weight of 2,400 kg/m^3 from Iran Beads Glass Beads Company were used to create a porous medium.

The porosity of glass beads was determined using both volume and weight methods. The average porosity of glass beads was 0.385. Freshwater needed for the experiments was obtained at 25°C and a density of 998 Kg/m^3 from the urban water supply network. Goswami and Clement (2007), Chang and Clement (2012), and Rezapour et al. (2018) used red food coloring to track the movement of the saltwater wedge in a porous medium. Thirty-five grams of sea salt was added to each liter of freshwater to prepare saltwater. A digital scale measured the density of dyed saltwater, and its value was 1,024 Kg/m^3.

The porous medium's hydraulic conductivity was measured on-site under different gradients using a method similar to that of Goswami and Clement (2007). To perform this method, first, a stable flow with a specific hydraulic gradient must be created in the aquifer system, then the hydraulic conductivity of the porous medium is calculated using Darcy's law. Therefore, first the porous medium of the laboratory model was completely saturated with freshwater, then the outlet drainage pipes in the left and right chambers were adjusted

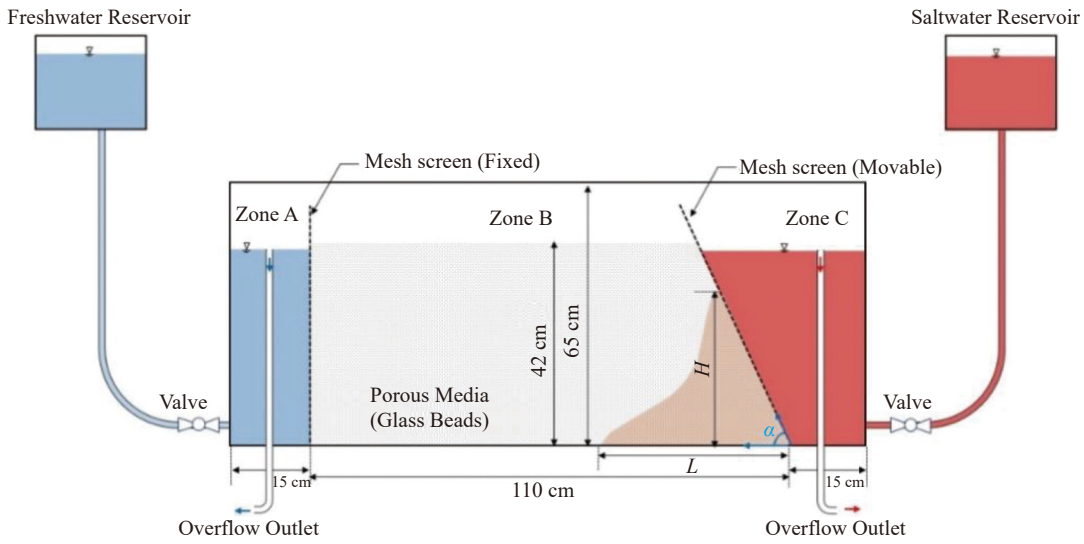

Fig. 2 Schematic diagram of the laboratory model

in such a way that the boundary conditions of the constant head in the side chambers, or in other words, the desired hydraulic gradient inside the aquifer, apply. To create a hydraulic gradient, freshwater was injected from the bottom of the left side chamber to allow the flow to pass through the porous medium, while the excess inflow water overflowed from a specified height through the drain pipe of the left chamber. As the flow passed through the porous medium, it was discharged through the drain pipe in the right chamber at a specific height.

After ensuring that the flow reached a stable condition, the volume of water coming out of the right chamber was measured with respect to time (flow rate). With the known values of flow rate, hydraulic gradient, and flow cross section, the value of hydraulic conductivity of the porous medium was measured by Darcy's equation. This process was repeated under different hydraulic gradients, and after averaging, the average value of hydraulic conductivity was estimated to be approximately 33 cm/min.

1.2 Experiment process

Considering that the purpose of this research was to investigate the effect of the slope of the beach on saltwater intrusion in an unconfined coastal aquifer, the desired beaches (presented in Table 1) were created by changing the angle of the mesh screen plate on the right side of the laboratory model. Therefore, before starting the experiment, the mesh plate on the right side of the laboratory model (saltwater side compartment) was set at 45° to create a beach with a slope of 45°. The glass beads were then poured into the central compartment in 5 cm layers under fully saturated conditions and compacted uniformly. By doing this, while distributing the glass beads evenly, the air bubbles trapped between the glass beads were removed from the porous medium. After completely saturating the porous medium with freshwater, the water level in the left side compartment of the model (freshwater) was adjusted to the level of 40.5 cm by the outlet vertical drain pipe. For the model to reach a stable condition, freshwater was injected from the bottom of the left lateral compartment so that while fixing the head at the level of 40.5 cm in this compartment, the flow passed through the porous medium and overflowed from the right lateral compartment, whose level was 37.4 cm.

Table 1 Details of experimental cases

Cases	Beach Slope
C1-90	90°
C2-75	75°
C3-60	60°
C4-45	45°

After the flow reached a stable condition, saltwater was injected into the right lateral compartment from the bottom. Saltwater replaced freshwater on the right side and overflowed from the 37.4 cm level through the vertical outlet drain pipe in that compartment. When saltwater was put in the right compartment, it made a wedge of saltwater in the middle compartment. Over time, the saltwater wedge advanced until finally, the flow reached a steady state, and the wedge did not advance through the porous medium after 15 minutes (the first stage of the experiment-SS1). Then, the level of freshwater in the left lateral compartment decreased from 40.5 cm to 39.5 cm. As expected, the saltwater wedge advanced again and continued to advance until a new stable condition was reached (the second stage of the experiment-SS2). In the experiment's last stage, the freshwater level was increased momentarily to 40.5 cm. As a result, the wedge returned to the saltwater side compartment until it reached a stable condition, and the regression of the saltwater wedge ceased (the third stage of the experiment-SS3).

To investigate the process of saltwater intrusion on beaches with slopes of 60°, 75°, and 90°, the mesh screen plate of the right side compartment of the laboratory model was adjusted to the desired angles, and all three stages of the above experiments were performed for these beaches as well as the 45° beach. Fig. 3 shows the images of the laboratory model on the desired slopes.

1.3 Image processing

In this research, an image processing technique was used to identify the behavior of saltwater intrusion in the porous medium and to calculate the characteristics of the saltwater wedge. Recently, many researchers have used image processing techniques to measure the parameters of laboratory models (Dalai et al. 2020; Dalai and Dhar, 2023; Rezapour et al. 2018). The process of saltwater intrusion in the central compartment was recorded using a PENTAX digital camera with a resolution of 3,368 × 6,000 pixels, which could capture images at specific time intervals. In all test stages, images were automatically taken from the flow tank (Zone B) at 60-second intervals. The

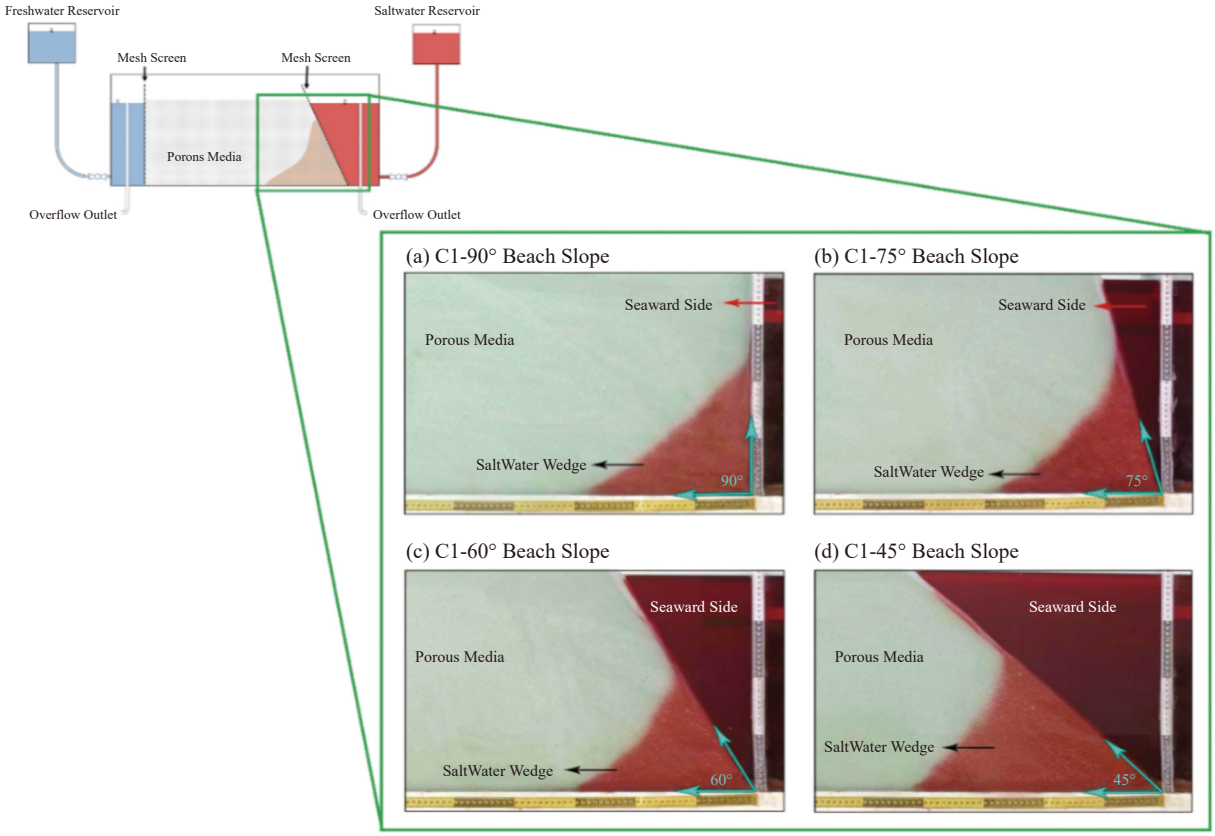

Fig. 3 Images of the laboratory model for different beach slopes

distance of the camera from the laboratory model and other parameters of the camera were set so that the boundary of the advancing zone of the saltwater wedge can be well identified. Also, in the pictures taken, in addition to the laboratory model, the glass boxes containing the porous medium with diluted saltwater (5%, 25%, 50%, 75%, and 95%) can be seen (Fig. 4). Hence, the camera was placed at a distance of 1.5 m from the laboratory model.

An image is displayed with its dimensions (height and width) based on the number of pixels. Images are created by combining multiple pixels, each holding color intensity information. An image can also be displayed in 3D, where x, y, and z are converted to spatial coordinates. The pixels are arranged in a matrix, known in this case as a Red, Green, Blue (RGB) image. Each pixel contains three integers between 0 and 255 (the integers

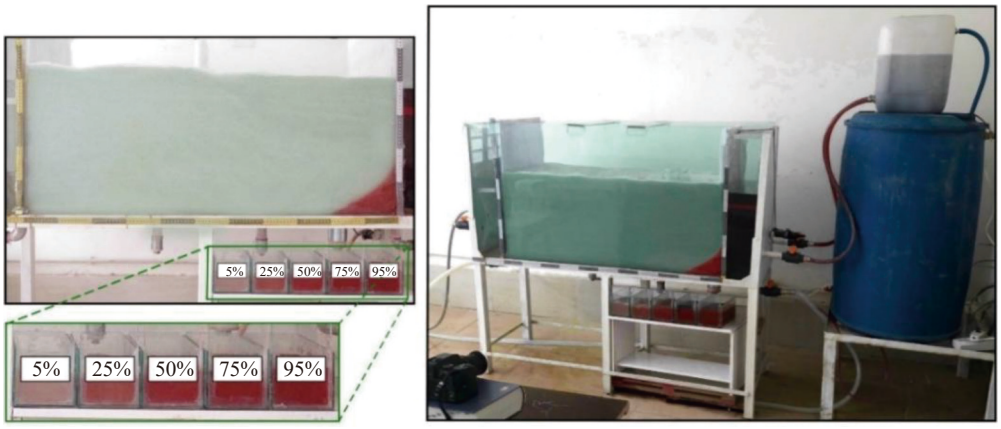

Fig. 4 Laboratory model with porous medium boxes with specific saltwater concentration fourth Steps

Note: After obtaining the numerical value equivalent to saltwater with a concentration of 50% ($C^{50\%}$) and the corrected pixel values of each model image at each time step ($C_{i,j}$), the contour lines of saltwater with 50% concentration were drawn in MATLAB software. After drawing the above contour line, the position of the toe of the saltwater wedge and the height of the wedge are determined.

represent the intensity of red, green, and blue colors). To extract the characteristics of the saltwater wedge, a relationship between the saltwater concentration space and the color intensity values of each pixel (red, green, and blue) should be obtained. In this research, the following steps were performed to process the images and derive the relationship between the concentration and color intensity of each pixel:

First Step: In this research, in all the experiments, pictures were automatically taken of saltwater's advancing and receding process at 60-second intervals. The images captured by the camera contain parts other than the central flow compartment (Zone B) that must be removed before processing. Since the saltwater solution is red using food coloring, the extraction of the saltwater intrusion zone can be easily separated. Therefore, the raw images were corrected and aligned using predefined static control points.

Second Step: After the preliminary analysis of the images in MATLAB software, it was observed that of the three main colors (RGB), the intensity of the blue color is always dominant, and the difference in the extent of the saltwater wedge is mainly influenced by the intensity of the red (R) and green (G) colors. Thus, to get the relationship between the saltwater concentration and the color intensity values of each pixel, a series of modifications are needed for the values of each pixel. According to the method proposed by Dalai et al. (2020), equation (1) was used to modify the values of each pixel of the images.

$$C_{i,j} = 255 + \left[D^{R}_{i,j} - D^{G}_{i,j}\right] \tag{1}$$

Where: $C_{i,j}$ are the modified values of each pixel of the primary image at locations i and j, $D^{R}_{i,j}$ and $D^{G}_{i,j}$ are the values of red and green color intensity, respectively. Each pixel in the original image is at positions i and j. Using MATLAB software and applying Equation (1), the numerical values of the pixels of all images were modified. Some noise was also observed regarding the color distribution of the modified images, which was somewhat reduced by applying the neighborhood average to the numerical values of the pixels of each image.

Third Step: In this research, the level curve with 50% diluted saltwater concentration was used as the boundary of the mixing zone of saltwater and freshwater to determine the characteristics of the saltwater wedge (length, height, and area) (Dalai et al. 2020; Dalai and Dhar, 2023; Rezapour et al. 2018; Robinson et al. 2015). To draw contour lines of equal concentration of the saltwater wedge, five glass boxes with length dimensions of 15 cm, height of 20 cm, and width of 40 cm were made. Using the dilution method, saltwater solution with diluted concentrations of 5%, 25%, 50%, 75%, and 95% were prepared and poured into each box along with glass beads (porous medium). Glass boxes were installed at the bottom of the central compartment of the model so that these boxes could be seen in all the pictures taken from the laboratory model (Fig. 4).

By applying equation (1) to the numerical values of pixels in the box range with 50% concentration in MATLAB software, the modified numerical values of pixels with 50% concentration ($C^{50\%}_{i,j}$) were determined. Then, according to Equation (2), the numerical value corresponding to 50% concentration was obtained by averaging the corrected values.

$$C^{50\%} = \frac{1}{MN}\sum_{j=1}^{N}\sum_{i=1}^{M} C^{50\%}_{i,j} \tag{2}$$

Where: M and N are, respectively, the numbers of pixels in the i and j directions of the image, $C^{50\%}_{i,j}$ is the corrected numerical value of each pixel at the i and j location, and $C^{50\%}$ is the numerical value of salinity equivalent to 50% concentration.

1.4 Numerical simulation

In this research, the SEAWAT finite difference model was used to simulate saltwater wedge advance experiments in a constructed laboratory model. Also, the groundwater flow equation and the pollutant diffusion and transfer equation are respectively solved by the MODFLOW software and the MT3DMS software (Zheng and Wang, 1999). In fact, this model predicts the flow head by coupling these two equations with density and pollutant concentration. The details of the equations and the method of discretization and solution have been described in many references, and we refrain from repeating them here. The SEAWAT model has recently been used to simulate saltwater intrusion (Abdoulhalik and Ahmed, 2017a; Noorabadi et al. 2017; Abdelgawad et al. 2018; Abdoulhalik and Ahmed, 2017b). To use the SEAWAT model, this study utilizes the GMS software package, as a graphical interface and pre-processor and post-processor for several groundwater models.

Due to the fact that square grid meshs are used in the finite difference method, this method is limited by the geometric and physical conditions of the studied area and the possible changes of these conditions. Thus, in order to increase the accuracy

of the model, smaller meshes can be used in sloping borders (curved borders). However, excessive mesh refinement does not necessarily improve accuracy; over small meshes increase the number of unknowns and may lead to numerical instability or reduced solution accuracy.

In this research, due to the effectiveness of dimensions in simulation accuracy, the Péclet number criterion of less than 4 has been used in the selection of numerical model network dimensions (Voss and Souza, 1987). According to this relationship, the dimensions of the grid cells along the length and height of the model are equal to 0.5 cm (ΔX=ΔZ=0.5 cm), and the width of the model is divided into 8 rows with a size of 5 cm (ΔY=5 cm). Considering the similarity in grain size and particle diameter between the glass beads in the porous medium and those in the Goswami and Clement (2007) research, a longitudinal dispersion coefficient of one millimeter was adopted in this study. Comparable small dispersivity values (of about a millimeter) have been previously reported for similar uniform porous media systems (Oswald and Kinzelbach, 2004). According to the research of Johannsen et al. (2002); Goswami and Clement (2007), the transverse dispersivity was considered to be 1/10 of the longitudinal dispersivity. Fig. 5 shows the conceptual model and boundary conditions used to simulate the numerical model.

According to the results of laboratory observations, the duration of each stage of the saltwater wedge advance and recede until reaching a steady state is 45 minutes. The time step for each of the three simulation stages was also set to Δt = 1 min. Table 2 shows a summary of the parameters used in the SEAWAT model to simulate the laboratory experiments.

2 Results and discussion

2.1 Laboratory analysis using image processing

This study evaluated the effect of beach slope on saltwater wedge dynamics in porous media. Three indices of the length, height, and area of the saltwater wedge, based on the contour line of 50% saltwater concentration were considered as the representative parameters of saltwater intrusion. Laboratory models, image processing techniques, and numerical simulations of laboratory observations were used to analyze the saltwater wedge's advance and recede behavior in coastal aquifers. As mentioned earlier, the experiments were carried out in three stages. Due to the neglect of the effects of boundary conditions at the beginning of the first stage of the experiment (SS-1), saltwater intrusion was not investigated in this stage. Only the stable condition of the first stage (SS-1) was used as the initial condition for the second stage of the experiment (SS-2) or saltwater intrusion. In the second stage (SS-2), the freshwater level in the left lateral compartment decreased from 40.5 cm to 39.5 cm, and in the third stage (SS-3) or wedge recede, the freshwater level returned to the initial state (40.5 cm).

The images of laboratory experiments and the results of the numerical model of the advance and recede of the saltwater wedge for the beach with a 90° slope and a 45° slope are respectively presented in Figs. 6 and 7. The contour line of saltwater with a concentration of 50% is marked with a black dashed line in the simulation images of the numerical model. In the images of laboratory

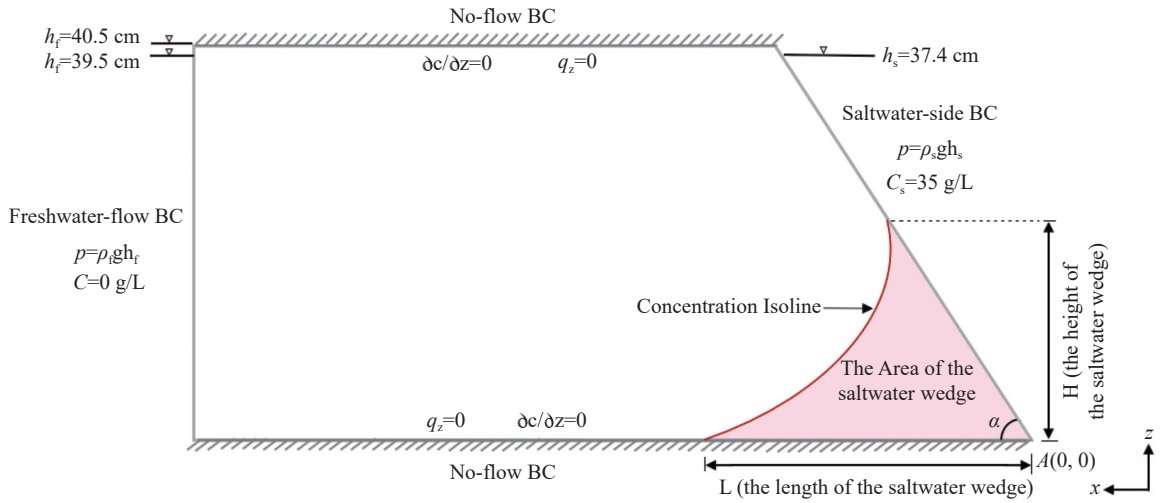

Fig. 5 Conceptual model and boundary conditions used to simulate the numerical model

Table 2 Summary of the numerical simulation parameters

Input parameters	Value	Unit
Domain length	110	cm
Domain height	42	cm
Domain width	40	cm
Hydraulic conductivity	33	cm/min
Longitudinal dispersivity	0.1	cm
Transversal dispersivity	0.01	cm
Freshwater density	998	g/L
Saltwater density	1024	g/L
Saltwater concentration	35	g/L
Porosity	0.385	-
Saltwater level	37.4	cm
Freshwater level	40.5 and 39.5	cm

observations, the above contour line obtained by the image processing technique is marked with a yellow line. The comparison of the results shows good agreement between the laboratory observations and the simulation results of the numerical model. However, the numerical model results show a greater curvature of the common border of saltwater and freshwater compared to the laboratory experiments, especially near the sea boundary.

As seen in Fig. 6, reducing the freshwater level at the beginning of the saltwater intrusion stage reduced the interaction forces applied by freshwater on the saltwater wedge. As a result, the balance in the laboratory model system was disrupted, and the saltwater wedge advanced again until reaching the new balance conditions (Fig. 6b). In the third stage (SS-3), as the freshwater level increased, the interaction forces applied by the freshwater on the wedge increased, and the wedge was pushed back towards the side compartment of the saltwater (sea) (Fig. 6c). A similar pattern is observed in Fig. 7; however, the shallower slope affects the curvature and dynamics of the wedge. This comparison clearly illustrates the effect of beach slope on the behavior of the saltwater wedge, and the difference in slope also influences the extent of the wedge's advance.

2.2 Numerical simulation and model validation

To validate the SEAWAT numerical model, the indices of saltwater wedge length (L), saltwater

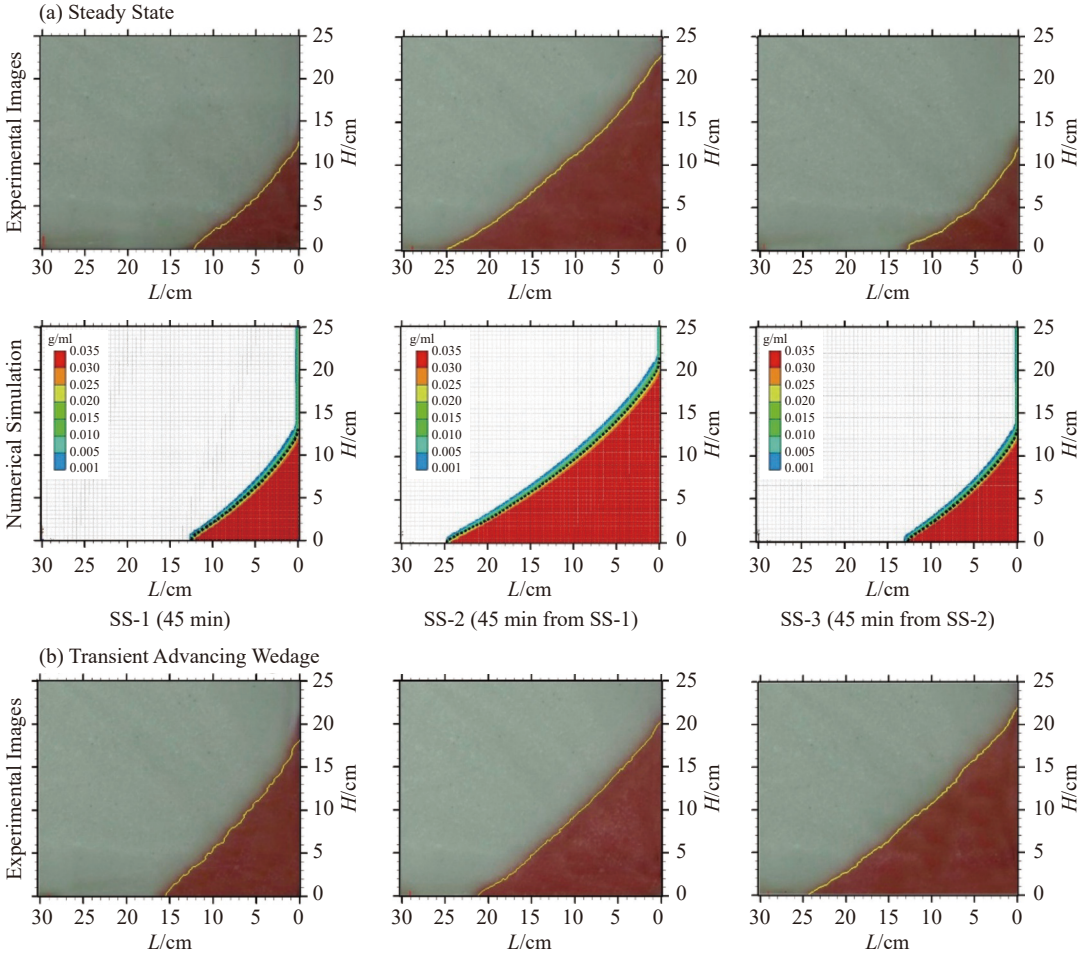

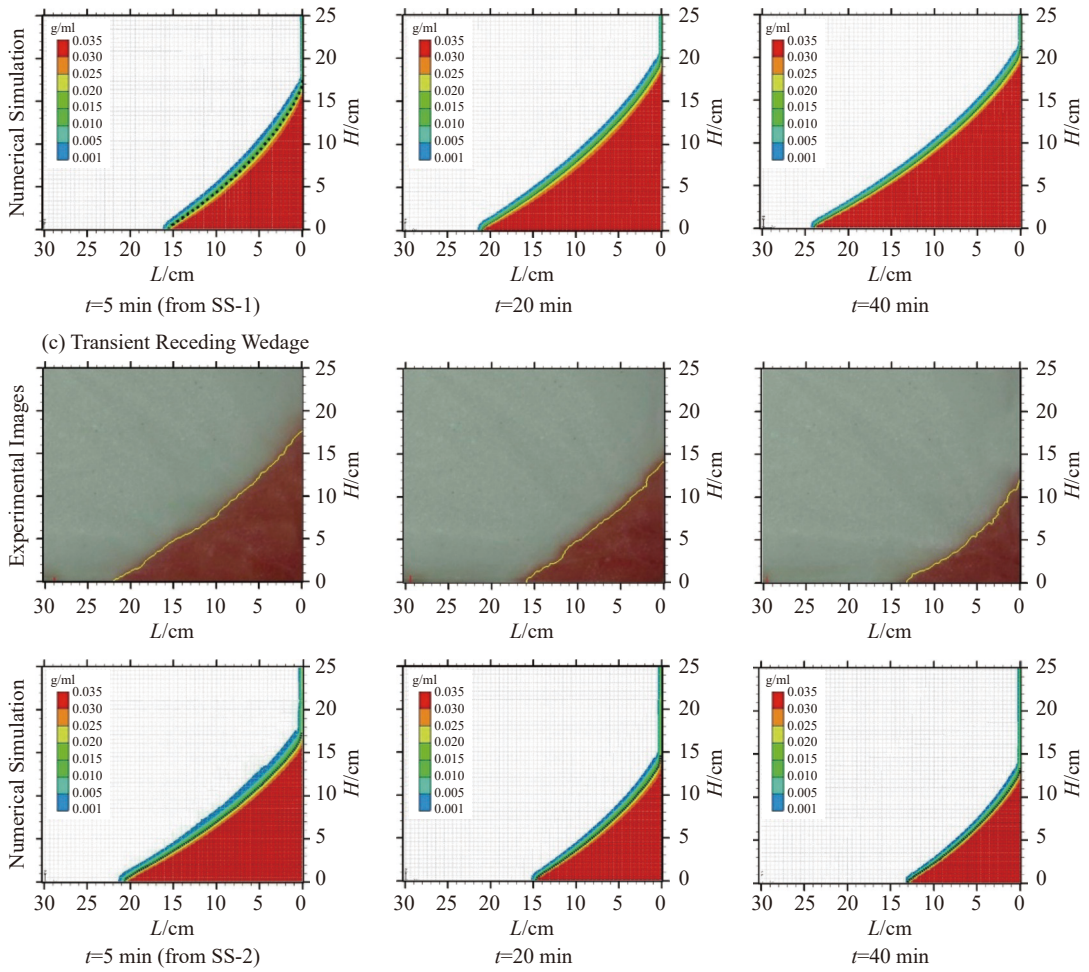

Fig. 6 Laboratory experiments and numerical simulations of the advancing and receding saltwater wedge for a 90° slope beach (C1-90)

wedge height (H), and saltwater wedge area (S) were measured using image processing techniques on images taken during the saltwater intrusion process at one-minute intervals. These measurements were then compared with the results of the numerical model simulation. The changes in the indices of saltwater wedge length (L), saltwater wedge height (H), and saltwater wedge area (S) on the beaches with the studied slopes are respectively presented in Figs. 8−10. Laboratory results were extracted at intervals of one minute (automatically) and numerical simulation were extracted at intervals of 5 minutes based on the contour line of 50% saltwater concentration. In Figs. 8−10, the ascending branch of each diagram corresponds to the advanc stage of the saltwater wedge (SS-2), and the descending branch corresponds to the receding stage of the saltwater wedge (SS-3).

Fig. 8 and Fig. 9 show good agreement between the experimental and numerical results for the toe length (L) and height (H) saltwater wedge indices. Fig. 10 shows a slight difference between the experimental data and the numerical simulation results for the area of the saltwater wedge (S). Nevertheless, the process of change in this index is similar for both numerical and laboratory modeling approaches under transient conditions. The reason for this difference can be explained by the lack of completely uniform properties in the porous medium and the lack of identical boundary conditions in the laboratory and numerical models, and the greater curvature of the common boundary of saltwater and freshwater in the results of the numerical model compared to the laboratory experiments, especially near the sea boundary. Robinson et al. (2015) stated that the reason for the linearity of the interface in laboratory models compared to numerical models is the presence of slight inhomogeneities in the porous medium (slight changes in the size and shape of beads).

2.3 Numerical model assessment

In this study, statistical indices such as the

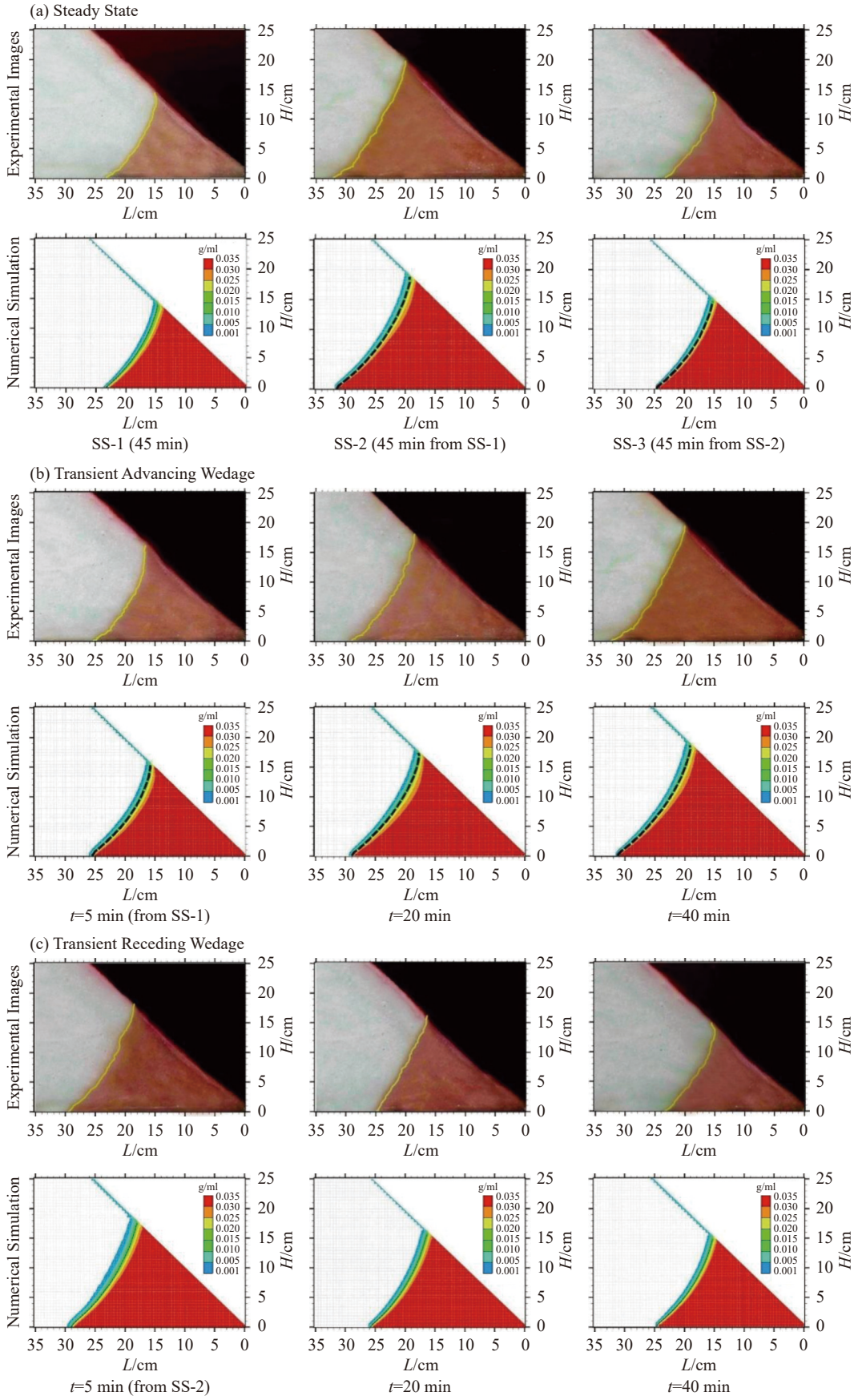

Fig. 7 Laboratory experiments and numerical simulations of the advancing and receding saltwater wedge for a 45° slope beach (C4-45)

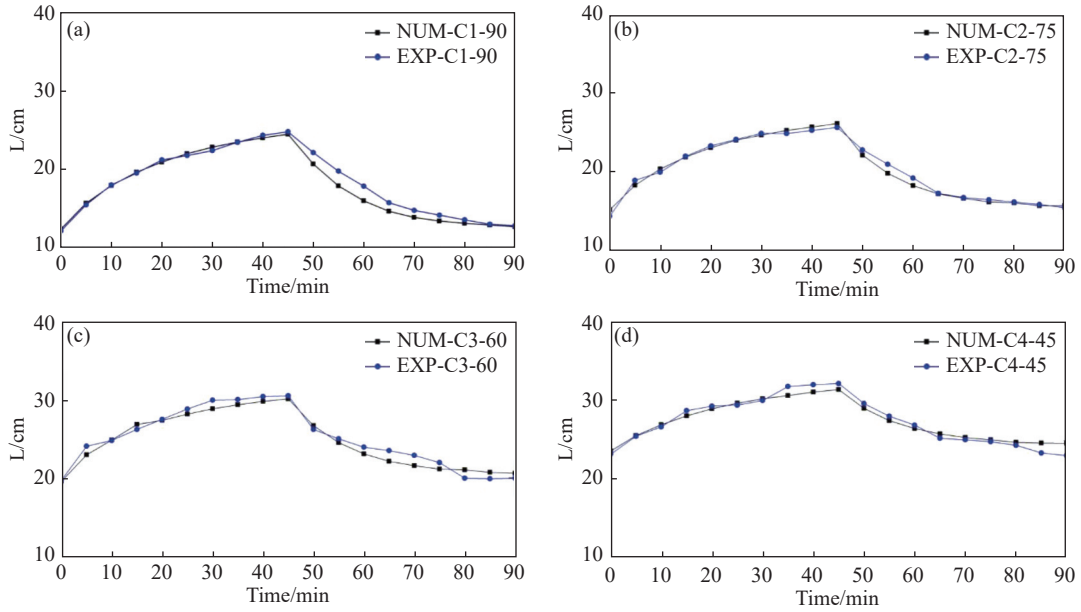

Fig. 8 Changes in the saltwater wedge toe length index for beaches with the desired slopes under transient conditions

(a) C1-90, (b) C2-75, (c) C3-60 (d) C4-45, The beginning of the wedge recede stage is from t=45 min

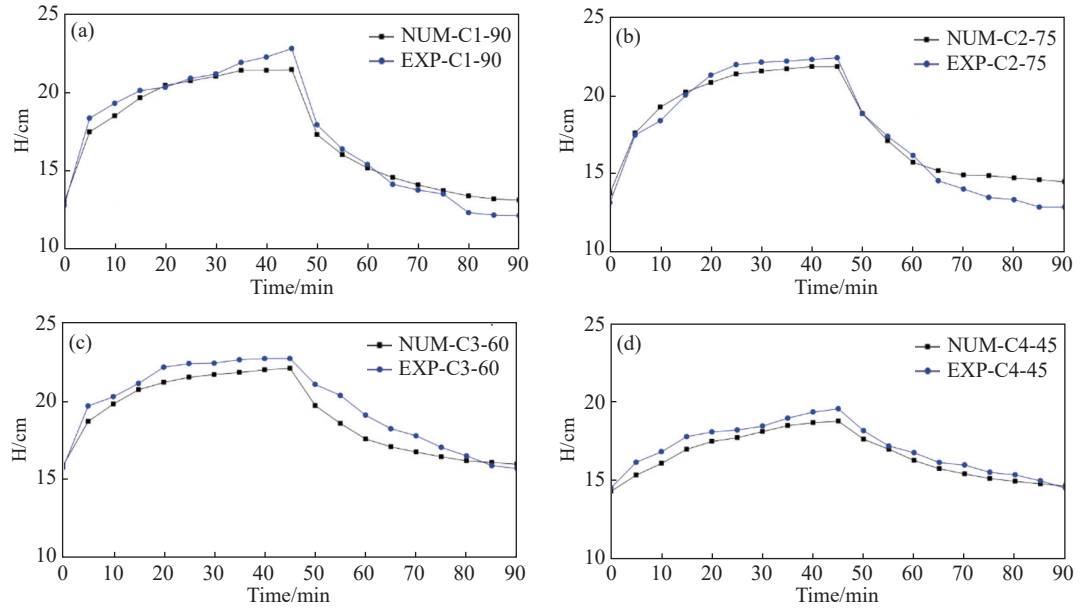

Fig. 9 Changes in the saltwater wedge height index for beaches with the desired slopes under transient conditions

(a) C1-90, (b) C2-75, (c) C3-60, (d) C4-45. The beginning of the wedge recede stage is from t=45 min

Nash–Sutcliffe efficiency (CE) and the correlation coefficient (R^2), according to Equations (3) and (4), were used to evaluate the numerical model for estimating the characteristics of the saltwater wedge. In the mentioned equations, n is the number of data points, O_i is the observed value (laboratory model) P_i is the predicted value (numerical model), $\overline{O}$ is the mean of the laboratory model values, $\overline{P}$ is the mean of the numerical model values, R^2 is the correlation coefficient, and CE is the Nash–Sutcliffe efficiency criterion. The optimal value of the correlation coefficient is 1. Moreover, the closer the Nash–Sutcliffe efficiency index is to one, the more accurate the model is.

$$R^2 = \left[\frac{\sum_{i=1}^{n} (O_i - \overline{O})(P_i - \overline{P})}{\sqrt{\sum_{i=1}^{n} (O_i - \overline{O})^2} \sqrt{\sum_{i=1}^{n} (P_i - \overline{P})^2}} \right]^2 \quad (3)$$

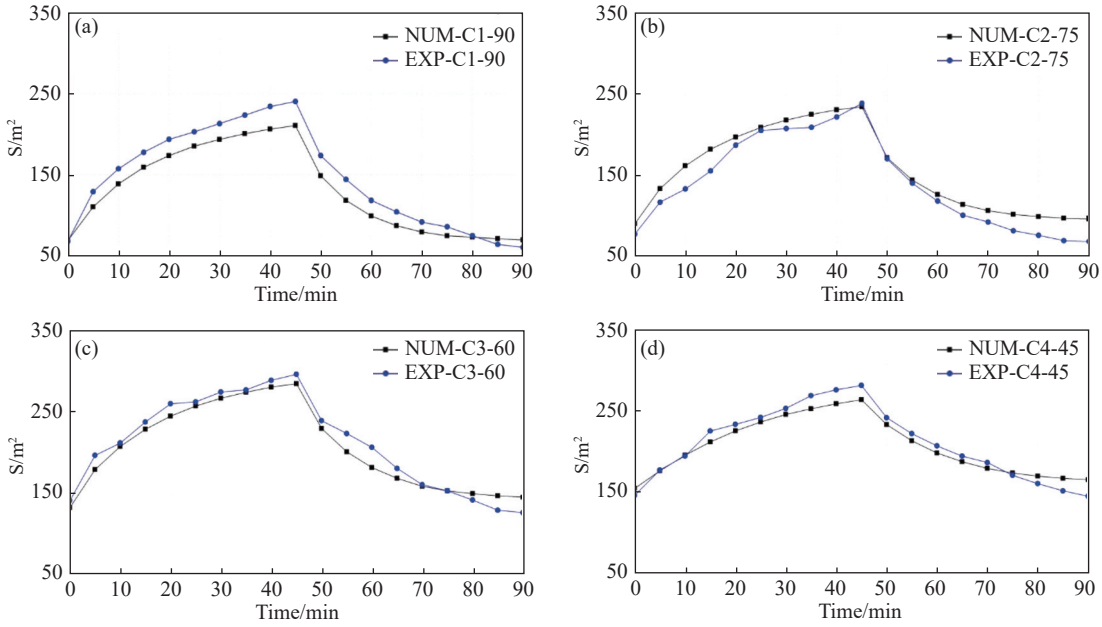

Fig. 10 Changes in the saltwater wedge area index for beaches with the desired slopes under transient conditions

(a) C1-90, (b) C2-75, (c) C3-60, (d) C4-45. The beginning of the wedge recede stage is from t=45 m

$$CE = 1 - \frac{\sum_{i=1}^{n}(O_i - P_i)^2}{\sum_{i=1}^{n}(O_i - \overline{O})^2} \quad (4)$$

The values of the statistical indices obtained from comparing the laboratory model and numerical model data during the intrusion and retreat stages of the saltwater wedge, in the experiments conducted to investigate seawater intrusion toward the coastal aquifer with the studied slopes, are presented in Table 3 and Table 4, respectively.

The statistical indices presented in Table 3 and Table 4 indicate that the SEAWAT numerical model demonstrates very high accuracy in estimating the position of the saltwater wedge during both the advance and recede stages. It can also be observed that among the saltwater wedge indices, the toe length index is estimated more accurately by the numerical model compared to the height and area indices.

Table 3 Statistical indices values during the advance stage of the saltwater wedge

Cases	Indicators of Saltwater Wedge	Statistical indicators	
		R^2	CE
C1-90	Toe length (L)	0.996	0.995
	Height (H)	0.974	0.938
	Area (S)	0.993	0.832
C1-75	Toe length (L)	0.985	0.983
	Height (H)	0.985	0.965
	Area (S)	0.971	0.896
C1-60	Toe length (L)	0.978	0.962
	Height (H)	0.987	0.881
	Area (S)	0.991	0.953
C1-45	Toe length (L)	0.977	0.953
	Height (H)	0.982	0.821
	Area (S)	0.992	0.929

Table 4 Statistical indices values during the recede stage of the saltwater wedge

Cases	Indicators of Saltwater Wedge	Statistical indicators	
		R^2	CE
C1-90	Toe length (L)	0.976	0.923
	Height (H)	0.991	0.940
	Area (S)	0.976	0.887
C1-75	Toe length (L)	0.977	0.970
	Height (H)	0.980	0.862
	Area (S)	0.990	0.889
C1-60	Toe length (L)	0.927	0.921
	Height (H)	0.925	0.784
	Area (S)	0.947	0.918
C1-45	Toe length (L)	0.973	0.922
	Height (H)	0.984	0.905
	Area (S)	0.970	0.917

2.4 Influence of beach slope and groundwater level changes

To investigate the effect of the beach slope on the dynamics of the saltwater wedge, the changes in

the toe length index of the saltwater wedge in the studied beaches during the process of advancing and receding the saltwater wedge in transient and stable conditions are shown in Figs. 11 and 12.

Figs. 11 and 12 show that although the change trend of saltwater wedge toe length index is similar for both numerical and laboratory modeling, there is a slight difference between the laboratory data and the numerical simulation results. The reason for this difference can be explained by the lack of completely uniform properties of the porous medium (the presence of slight inhomogeneities in the porous medium, including slight changes in the size and shape of the particles). Also, at the beginning of each stage of the saltwater wedge advance and recede, it took about 2

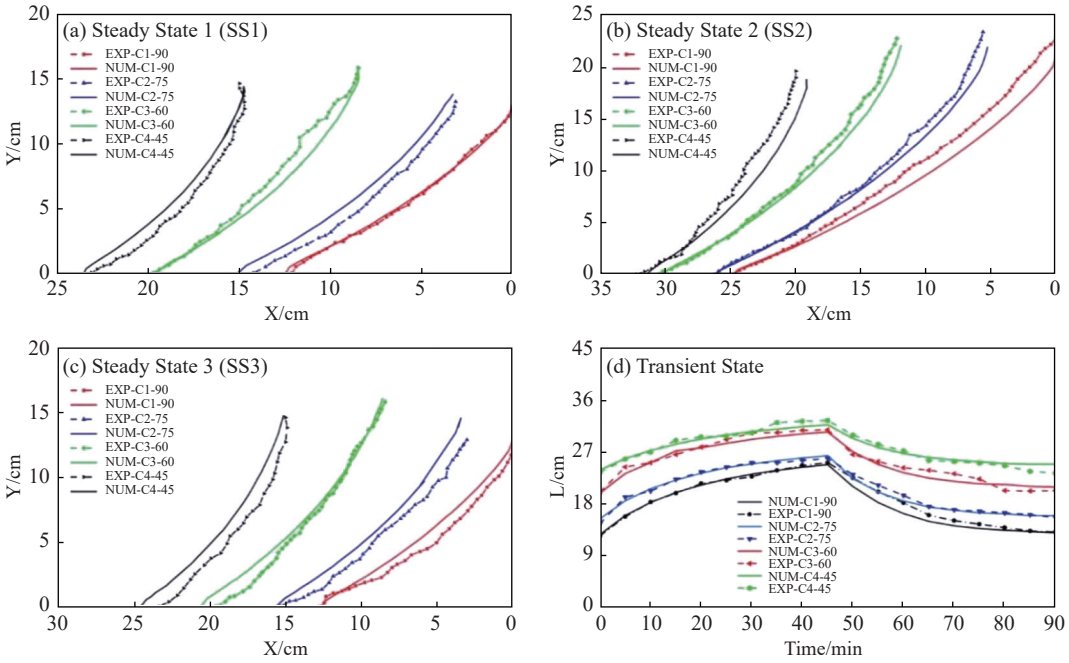

Fig. 11 Changes in the toe length index of the saltwater wedge for beaches with different slopes during the advance and recede stages of the wedge

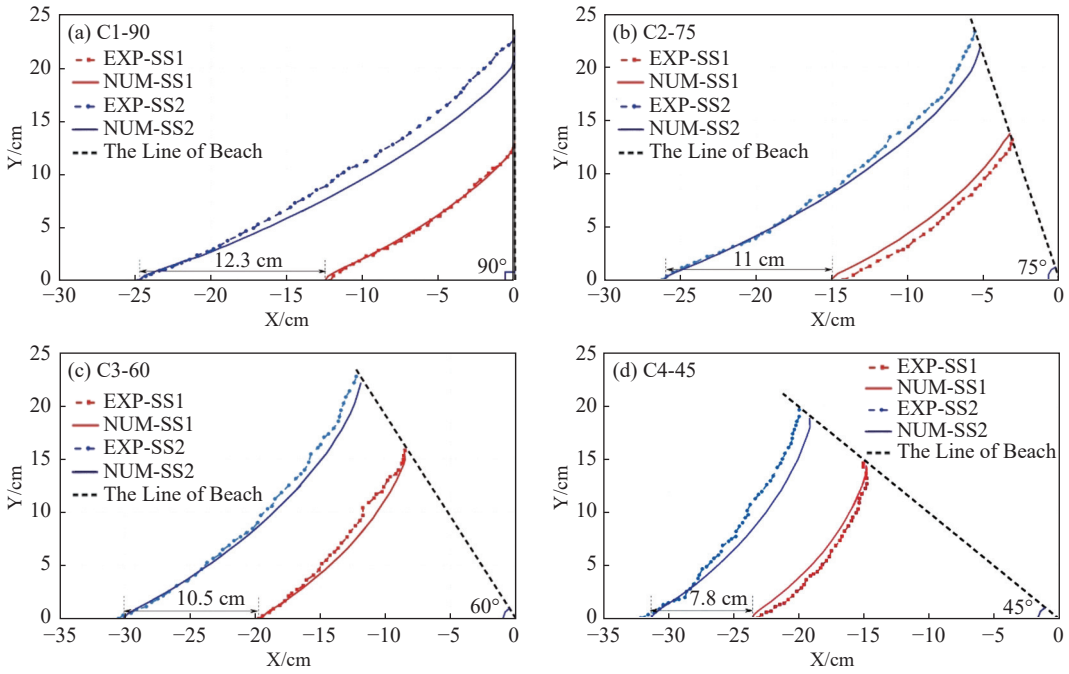

Fig. 12 Changes in the saltwater wedge toe length index during the advancing process of (a) C1-90, (b) C2-75, (c) C3-60, and (d) C4-45

minutes to adjust the freshwater level in the left side chamber of the laboratory model to be completely adjusted and fixed at the desired level. Therefore, some of the initial delays observed between the experimental data and numerical simulation results may be related to this experimental problem (lack of fully identical boundary condition effects in experimental and numerical models).

As seen in Fig. 11, the position of the toe of the saltwater wedge on the 45° beaches in both the advance and recede stages is more distant from the saltwater boundary of the sea than that of the other studied beaches. In other words, the steeper the beach, the shorter the length of the saltwater wedge toe. Ataie-Ashtiani et al. (1999), Liu et al. (2012), Walther et al. (2017) and Dalai and Dhar (2023) reached this conclusion in their studies. The cause of this behavior can be described as the change in the angle of the mesh screen plate of the right side compartment of the laboratory model from 90° to 45°. The pressure field exerted by saltwater increased (increasing the force exerted by saltwater). Therefore, due to the difference in the density of saltwater and freshwater, a larger volume of saltwater moves from the sea boundary towards the aquifer, and the toe of the saltwater wedge advances more.

Also, the changes in the advancing length of the wedge toe due to the reduction of the freshwater level in the second stage of the experiment (SS-2) in the studied beaches are presented in Fig. 12. According to Fig. 12(a), in the second stage of the experiment (advancement stage of the wedge), on the beach with a 90° slope, the toe of the saltwater wedge advanced 12.3 cm compared to the stable conditions of the first stage of the experiment (SS-1). While in the same conditions, the advance distance of the wedge toe on the beach with a 45° slope was 7.8 cm, 4.5 cm less than the beach with a 90° slope. Therefore, in transient conditions, after the reduction of the freshwater level, it was observed that the displacement of the saltwater wedge on the vertical beach is about 57% more than on the beach with a slope of 45°, but after the process of advancing the wedge was stopped and the new steady state was reached, it was observed that despite the greater advance of the wedge toe on the 90° beach, the size of the saltwater wedge on the vertical beach was still smaller than that on the 45° beach.

2.5 Relative index displacement and intrusion indicators

A more accurate look at Figs. 8 to 10 shows that the behavior of the indicators of the wedge length, the height, and the area of the saltwater wedge in the advance and recede stages of the saltwater wedge differ from each other on different beaches. The relative displacement parameter of each index (the displacement of each index divided by the total change of that index), as a dimensionless parameter which provides the possibility of comparison independent of the unit and the size of the total change, was used to further investigate this issue. Equation (5) defines the relative displacement of each index in transient conditions.

$$a^*(t) = \frac{|a(t_s) - a(t)|}{\Delta a} \tag{5}$$

Where: $a^*(t)$ is the relative displacement of the index after t minutes from the start of each stage of the advance and recede of the saltwater wedge. Also, $a(t_s)$ is the size of each index in the steady state of each stage, and $a(t)$ is the size of each index after t minutes from the beginning of each stage. Δa is the total change of the desired index in each stage. Each of the three indices of toe length, height, and area of the saltwater wedge can replace the variable a in Equation (5).

The relative displacement of toe length and height indices of the saltwater edge in the studied beaches are shown in Figs. 13 and 14, respectively. Fig. 13 shows that the index of wedge toe length reaches stable conditions earlier in the wedge recede stages (SS-3) than in the advance stages (SS-2). It was also observed that in all studied beaches, the time to reach stable conditions in the return stages is approximately 7 minutes earlier than the time to reach stable conditions in the advance stages of the wedge. This phenomenon was reported in experimental and numerical studies by Chang and Clement (2012), Lu and Werner (2013), Robinson et al. (2015), and Rezapour et al. (2018).

According to the results presented in Fig. 14, it was found that, unlike the index of the wedge's length, which reaches stable conditions faster in the recede stages than in the advance stage, the index of the wedge's height in all the studied beaches in both the advance and recede stages is approximately equal at stable conditions. Rezapour et al. (2018) also presented this result in their study.

To provide a more detailed assessment of the seawater wedge behavior in the studied beaches, the relative displacements of the wedge toe length, height, and area indices during the advance and recede stages of the wedge were presented together in a single figure, as shown in Figs. 15 and 16,

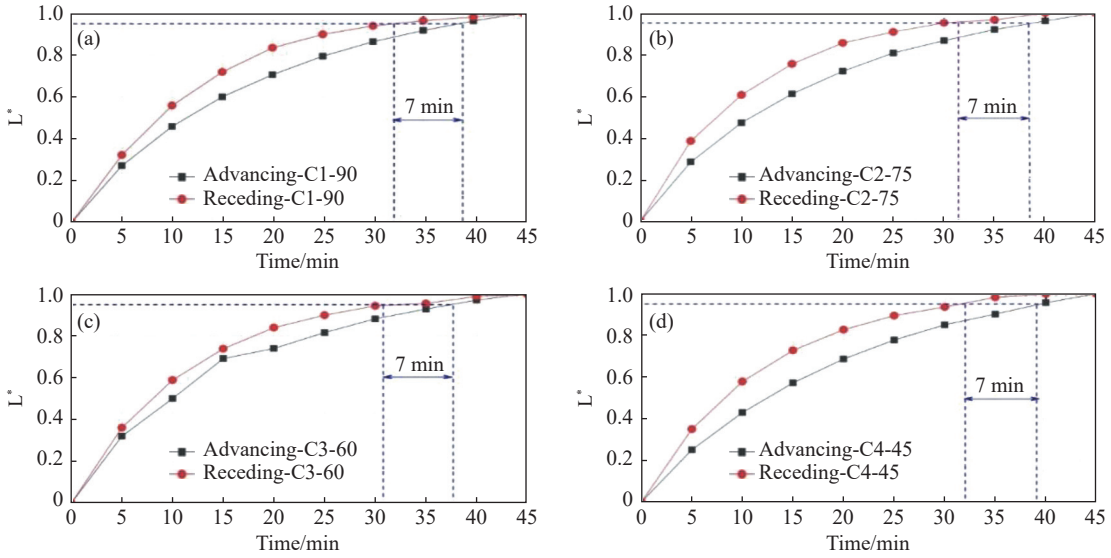

Fig. 13 Changes in the relative displacement of the toe length of the saltwater wedge in the advance and recede stages (a) C1-90, (b) C2-75, (c) C3-60, (d) C4-45

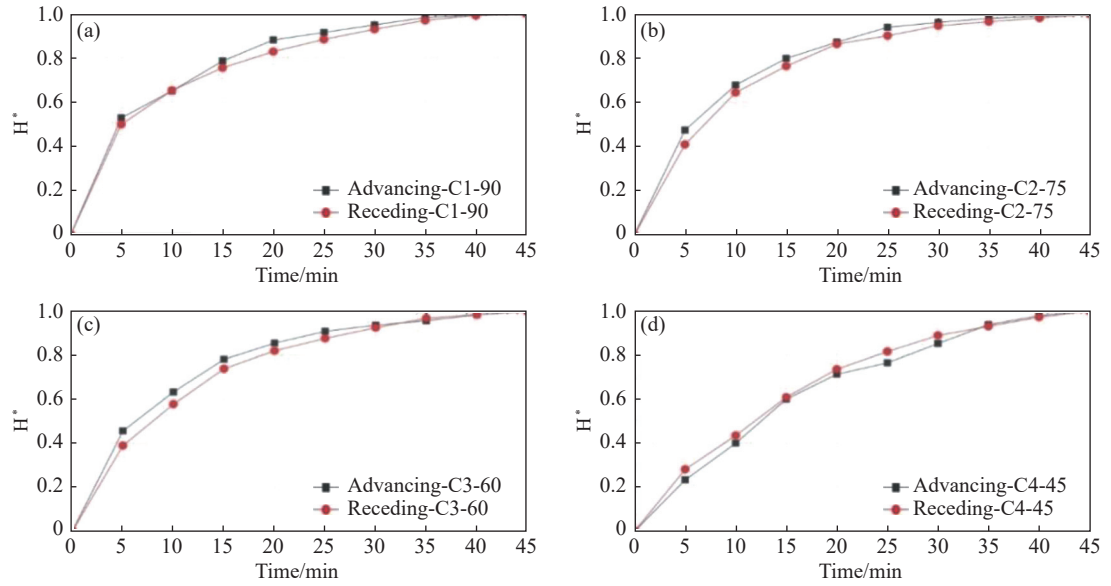

Fig. 14 Changes in the relative displacement of the height of the saltwater wedge in the advance and recede stages (a) C1-90, (b) C2-75, (c) C3-60, (d) C4-45

respectively. This approach made it possible to compare the relative variations of each index at different times. Fig. 15 indicates that, in all the studied beaches, the relative rate of change in wedge area is comparable to the relative rate of change in wedge toe length during most time intervals. Therefore, the results obtained from this research show that the wedge toe length index, in addition to steady-stage conditions, can be a suitable representative for expressing the amount of saltwater entering the coastal aquifer in transient conditions.

Another noteworthy point is the behavior of the saltwater wedge height index under transient conditions. In the advancing stage (Fig. 15), the height of the wedge moves towards stability with a much higher relative speed compared to the toe and the area of the wedge, and it reaches stable conditions much earlier than them. While in the receding stage (Fig. 16), all three indicators stop almost simultaneously. The cause of this behavior can be described as the reduction in freshwater level in the left lateral compartment decreasing the freshwater pressure field. Therefore, saltwater is brought from the sea boundary towards the aquifer, and the interface starts to advance. Due to the

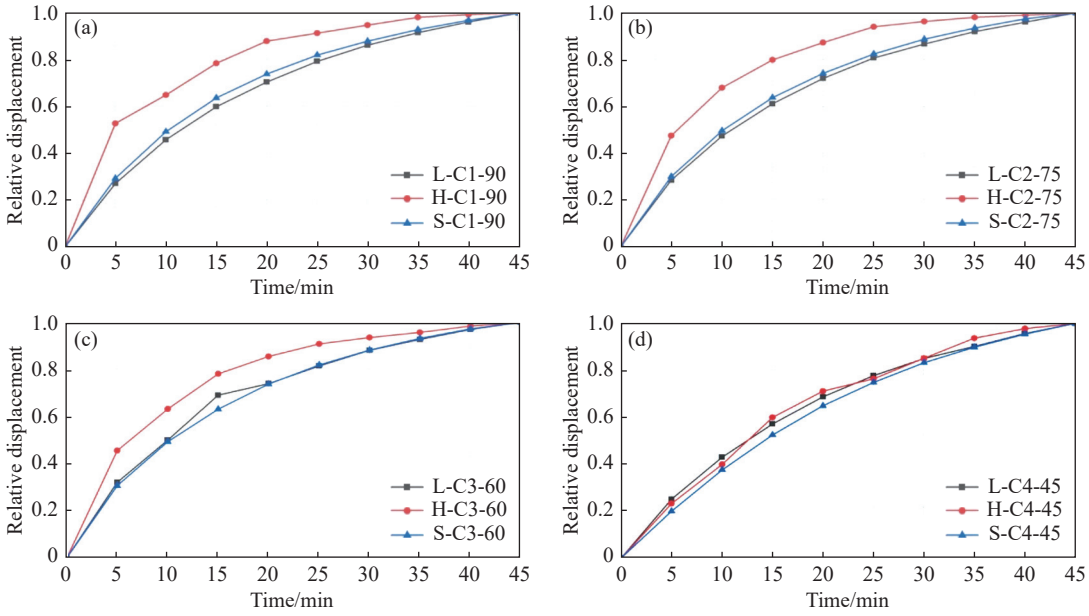

Fig. 15 Changes of selected indicators of saltwater wedge over time in the advance stage

(a) C1-90, (b) C2-75, (c) C3-60, (d) C4-45

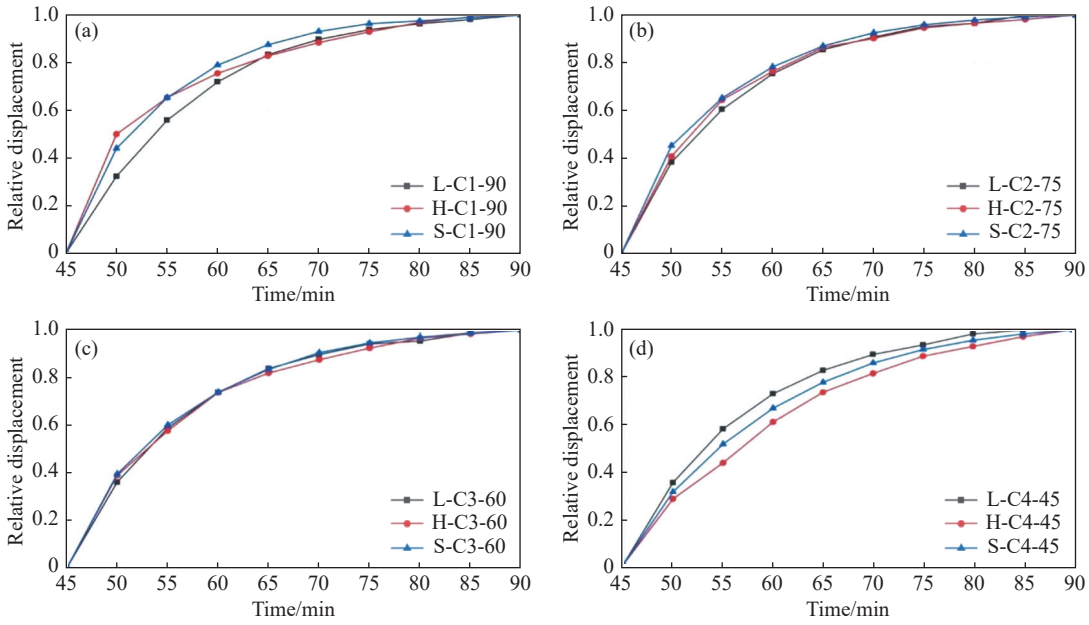

Fig. 16 Changes in selected indicators of the saltwater wedge over time in the recede stage

(a) C1-90, (b) C2-75, (c) C3-60, (d) C4-45

density difference between saltwater and freshwater, as the interface's depth increases, the advancement rate increases. As the advance rate of the interface increases, its relative advance rate decreases. Therefore, the height of the wedge, as the highest point of the interface, starts to move at the highest relative rate and reaches a stable condition earlier than other points of the interface. Accordingly, the wedge toe, as the lowest point of the interface, has the greatest final advance; as a result, with the lowest relative displacement rate, it reaches stable conditions later than other interface points.

In the receding stage of the wedge, because the index of the height of the wedge is located on the sea boundary, at the beginning of the receding stage, it decreases with a higher relative speed than the other two indices. Over time, freshwater currents enter the mixing zone and begin to wash away the thick layers of the mixing zone. Then, the flow of brackish waters created in the mixing zone moves along the interface towards the outlet of the

flow (on the sea boundary). The outflow of brackish waters from the sea border reduces the rate of the wedge height drop. The washing process continues until the wedge toe approaches a steady state. As a result, all three indicators of wedge toe length, area, and height reach stable conditions almost simultaneously.

2.6 Time to steady state across different slopes

In order to more closely examine the effect of the slope of the beach on the behavior of the saltwater wedge in the advance and recede stages, the trend of changes in the indices of toe length, height, and area of the saltwater wedge are shown in a single figure (Fig. 17). According to the trend of changes of all three indicators of toe length, height, and area of the saltwater wedge (Fig. 17), it can be seen that the time to reach stable conditions is longer on flatter slopes than on steeper slopes, which is consistent with the results of Walther et al. (2017).

2.7 Comparison with previous studies

In the following, the results of this research were compared with the results of Dalai and Dhar (2023) and Liu et al. (2012). Dalai and Dhar (2023) using the FEFLOW numerical model and developing a two-dimensional laboratory model and creating beaches with slopes of 15°, 20°, 25° and 30° and also Liu et al. (2012) using the FEFLOW numerical model and creating beaches with slopes of 15°, 30°, 45°, 60°, 75° and 90°, were investigated the effects of seawater tides and changes in the beach slope on the advance of seawater. A more accurate look at Fig. 11 shows that the behavior of the saltwater wedge in the advance and recede stages in the studied beaches is different from each other. To further investigate this issue, the parameter of the relative intrusion length (the toe length of the saltwater wedge divided by the saltwater level), as a dimensionless parameter which provides the possibility of comparison independent of the unit, was used.

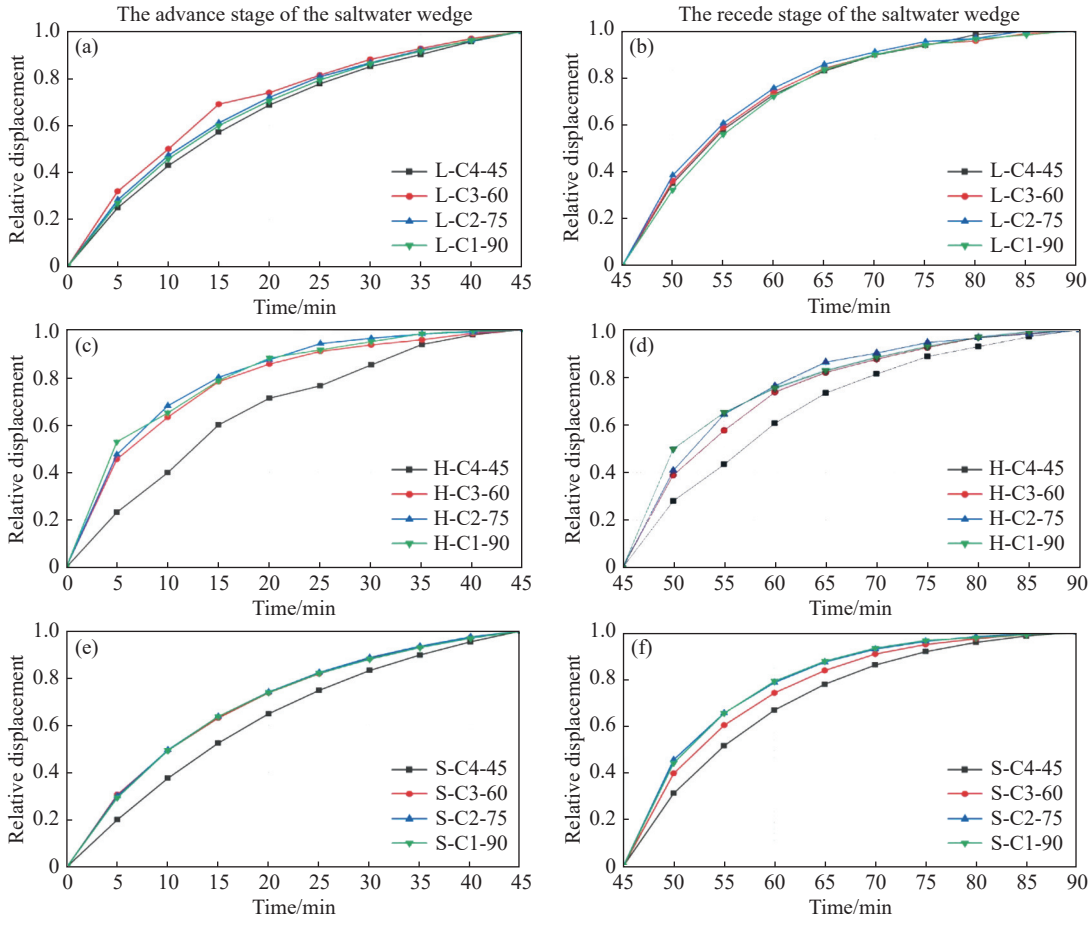

Fig. 17 Changes in saltwater wedge indices for beaches with desired slopes in transient conditions

Notes: (a) the toe length of the wedge in the advance stage, (c) the height of the wedge in the advance stage, (e) the area of the wedge in the advance stage, (b) the toe length of the wedge in the recede stage, (d) the height of the wedge in the recede stage, (f) the area of the wedge in the recede stage

Equation (6) defines the relative intrusion length.

$$\lambda = \frac{L}{H_s} \tag{6}$$

Where: λ is the relative length of the saltwater wedge intrusion, L is the toe length of the saltwater wedge, and H_s is the saltwater level (in the right compartment). The relationship between the relative length of the saltwater wedge intrusion (λ) and the beach angle (α) based on the results of the study by Dalai and Dhar (2023), Liu et al. (2012) and the results of this research in the initial steady state (SS-1), the steady state after the intrusion of the saltwater wedge (SS-2) and the steady state after wedge receding (SS-3) is shown in Fig. 18. According to Fig. 18, it can be seen that based on the results of this research, the rate of saltwater wedge intrusion is higher on milder beaches, and this is consistent with the research results of Dalai and Dhar (2023) and Liu et al. (2012). Also, the effect of the slope of the coast on the intrusion of the saltwater wedge can be expressed in the form of a logarithm function. Ataie-Ashtiani et al. (1999) also found that the influence of the tide on the intrusion length is much greater at a sloping beach than at a vertical one.

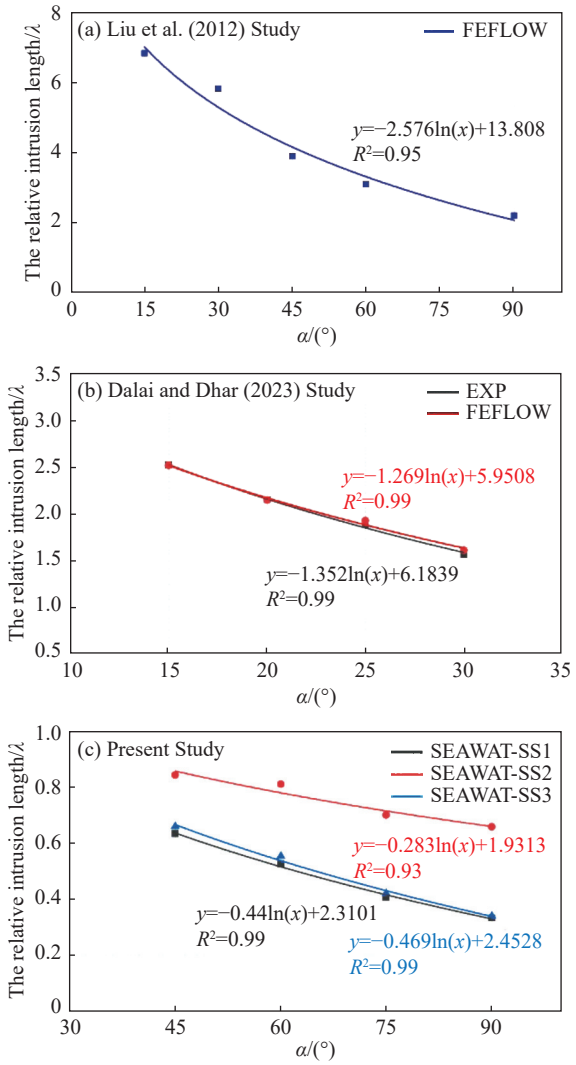

Fig. 18 Relationships between the relative intrusion length (λ) and the beach angle (α)

(a) The results of Liu et al. (2012) research, (b) The results of this research in steady state conditions

3 Conclusion

In this research, the effect of beach slope on seawater intrusion in unconfined coastal aquifers was investigated using a three-dimensional laboratory model, quantitative image processing, and numerical simulation with the SEAWAT model. The integrated use of these methods overcomes the limitations of manual observation and data extraction in laboratory experiments, providing a clearer and more accurate understanding of the saltwater wedge behavior under both steady and transient conditions.

The results showed that beach slope has a significant influence on both the spatial extent and temporal response of the seawater wedge. Gentler slopes cause greater inland intrusion of saltwater, while steeper slopes lead to more rapid system adjustment following hydraulic perturbations. These findings confirm that shoreline geometry plays an important role in determining both the equilibrium position and dynamic evolution of the saltwater–freshwater interface.

A key finding of this study is that the wedge toe length index can be considered a reliable indicator for estimating the magnitude and temporal development of seawater intrusion under both steady and transient conditions. In addition, the logarithmic relationship identified between the relative wedge length (λ) and the beach slope angle (α) provides a simple yet effective tool for assessing the influence of coastal slope in hydrogeological assessments. Overall, the outcomes of this research improve the understanding of how coastal morphology controls seawater intrusion dynamics and can assist in vulnerability evaluation and management planning of coastal aquifers.

References

Abarca E, Carrera J, Sanchez-Vila X, et al. 2007. Quasi-horizontal circulation cells in 3D seawater intrusion. Journal of Hydrology, 339: 118−129. DOI：10.1016/j.jhydrol.2007.02.017.

Abd-Elaty I, Polemio M. 2023. Saltwater intrusion management at different coastal aquifers bed slopes considering sea level rise and reduction in fresh groundwater storage. Stochastic Environmental Research and Risk Assessment, 37: 2083−2098. DOI：10.1007/s00477-023-02381-9.

Abdelgawad AM, Abdoulhalik A, Ahmed AA, et al. 2018. Transient investigation of the critical pumping rate in a laboratory-scale coastal aquifer. Water Resources Management, 32: 3563−3577. DOI：10.1007/s11269-018-1988-3.

Abd-Elhamid HF, Javadi AA. 2011. A cost-effective method to control seawater intrusion in coastal aquifers. Water Resources Management, 25: 2755−2780. DOI：10.1007/s11269-011-9837-7.

Abd-Elhamid HF, Sherif MM. 2020. Effects of aquifer bed slope and sea level on saltwater intrusion in coastal aquifers. Hydrology, 7(1): 5. DOI：10.3390/hydrology7010005.

Abdoulhalik A, Ahmed A, Abdelgawad A, et al. 2022. The impact of a low-permeability upper layer on transient seawater intrusion in coastal aquifers. Journal of Environmental Management, 307: 114602. DOI：10.1016/j.jenvman.2022.114602.

Abdoulhalik A, Ahmed AA. 2017a. The effectiveness of cutoff walls to control saltwater intrusion in multi-layered coastal aquifers: Experimental and numerical study. Journal of Environment Management, 199: 62−73. DOI：10.1016/j.jenvman.2017.05.040.

Abdoulhalik A, Ahmed AA. 2017b. Transient investigation of saltwater upconing in a laboratory-scale coastal aquifer. Estuarine Coastal and Shelf Science, 214: 149−160. DOI：10.1016/j.ecss.2018.09.024.

Ataie-Ashtiani B, Volker RE, Lockington DA. 1999. Tidal effects on sea water intrusion in unconfined aquifers. Journal of Hydrology, 216: 17−31. DOI：10.1016/S0022-1694(98)00275-3.

Ataie-Ashtiani B, Werner A, Simmons C, et al. 2013. How important is the impact of land surface inundation on seawater intrusion caused by sea-level rise? Hydrogeology Journal, 21: 1673−1677. DOI：10.1007/s10040-013-1021-0.

Cao X, Li Y, Wang Z, et al. 2024. Experimental and SEAWAT numerical study on seawater intrusion patterns in relation to beach slope and sea-level changes. Water, 16(3457): 1−15.

Chang SW, Clement TP. 2012. Experimental and numerical investigation of saltwater intrusion dynamics in flux-controlled groundwater systems. Water Resources Management, 48: 1−10. DOI：10.1029/2012WR012134.

Cheng ZS, Su C, Wang WZ, et al. 2026. Hydrogeological flow patterns and hydrochemical driving forces of groundwater in a typical coastal hilly region of the Jinjiang watershed, Southeast China: Recommendations for water pollution control and management. China Geology, 9(2): 1−17. DOI：10.31035/cg2024185.

Dalai C, Dhar A. 2023. Impact of beach face slope variation on saltwater intrusion dynamics in the unconfined aquifer under tidal boundary conditions. Flow Measurement and Instrumentation, 89: 102298. DOI：10.1016/j.flowmeasinst.2022.102298.

Dalai C, Munusamy SB, Dhar A. 2020. Experimental and numerical investigation of saltwater intrusion dynamics on sloping sandy beach under static seaside boundary condition. Flow Measurement and Instrumentation, 75: 101794. DOI: 10.1016/j.flowmeasinst.2020.101794

Deng B, Zhang W, Yao Y, et al. 2022. A laboratory study of the effect of varying beach slopes on bore-driven swash hydrodynamics. Frontiers in Marine Science, 9: 956379. DOI：10.3389/fmars.2022.956379.

Fang Y, Zheng T, Wang H, et al. 2021. Experimental and numerical evidence on the influence of tidal activity on the effectiveness of subsurface dams. Journal of Hydrology, 603: 127149. DOI：10.1016/j.jhydrol.2021.127149.

Flowers TC, Hunt JR. 2007. Viscous and gravitational contributions to mixing during vertical brine transport in water-saturated porous media. Water Resources Management, 43(1): W01407. DOI：10.1029/2005WR004773.

Goswami RR, Clement TP. 2007. Laboratory - scale investigation of saltwater intrusion dynamics. Water Resources Management, 43(4): W04418. DOI：10.1029/2006WR005151.

Gao C, Kong J, Wang J, et al. 2023. Combined

effect of subsurface dam and layered heterogeneity on groundwater flow and salinity distribution in stratified coastal aquifers. Acta Oceanologica Sinica, 42(8): 49−60. DOI：10.1007/s13131-023-2255-x.

Guo W, Bennett GD. 1998. SEAWAT version 1.1: A computer program for simulation of groundwater flow of variable density. Missimer International Inc, Fort Myers.

Johannsen K, Kinzelbach W, Oswald S, et al. 2002. The salt-pool benchmark problem Numerical simulation of saltwater upconing in a porous medium. Advances in Water Resources, 25(3): 335 – 348.

Kolditz O, Görke UJ, Shao H, et al. 2016. Thermo-Hydro-Mechanical chemical processes in fractured porous media: Modelling and benchmarking. Springer International Publishing. DOI: 10.1007/978-3-319-29224-3

Li FL, Chen XQ, Liu CH, et al. 2018. Laboratory tests and numerical simulations on the impact of subsurface barriers to saltwater intrusion. Natural Hazards, 91: 1223−1235. DOI：10.1007/s11069-018-3176-4.

Liu Y, Shang SH, Mao XM. 2012. Tidal effects on groundwater dynamics in coastal aquifer under different beach slopes. Journal of Hydrodynamics, 24: 97−106. DOI：10.1016/S1001-6058(11)60223-0.

Lu C, Xin P, Kong J, et al. 2016. Analytical solutions of seawater intrusion in sloping confined and unconfined coastal aquifers. Water Resources Research, 52(9): 6989−7004. DOI：10.1002/2016WR019101.

Lyu P, Song J, Wu J, et al. 2021. A numerical simulation study for controlling seawater intrusion by using hydraulic and physical barriers. Hydrogeology and Engineering Geology, 48(4): 32−40. (in Chinese) DOI：10.16030/j.cnki.issn.1000-3665.202007068.

Mazi K, Koussis AD, Destouni G. 2013. Tipping points for seawater intrusion in coastal aquifers under rising sea level. Environmental Research Letters, 8(1): 1−6. DOI：10.1088/1748-9326/8/1/014001.

Nam B, Solorzano-Rivas C, Jazayeri A, et al. 2025. Tidal, freshwater-saltwater interactions: Three-dimensional sand-tank experiments. Journal of Hydrology, 653: 132696. DOI：10.1016/j.jhydrol.2025.132696.

Narayanan D, Eldho TI. 2025. Investigations on the saline groundwater pumping method and its impact on active saltwater intrusion on a layered aquifer system. Journal of Environmental Management, 373: 123747. DOI：10.1016/j.jenvman.2024.123747.

Noorabadi S, Sadraddini AA, Nazemi AH, et al. 2017. Laboratory and numerical investigation of saltwater intrusion into aquifers. Journal of Materials and Environmental Science, 8(12): 4273−4283. DOI：10.26872/jmes.2017.8.12.450.

Oswald SE, Kinzelbach W. 2004. Three-dimensional physical benchmark experiments to test variable-density flow models. Journal of Hydrology, 290: 22−42. DOI：10.1016/j.jhydrol.2003.11.037.

Rezapour AB, Saghravani SFA, Ahmadifard AR. 2018. Studying the phenomenon of saltwater inflow to coastal aquifers in transient conditions using image processing and numerical modeling. Journal of Iranian Hydraulic Association.

Robinson G, Hamill G, Ahmed AA. 2015. Automated image analysis for experimental investigations of salt water intrusion in coastal aquifers. Journal of Hydrology, 530: 350−360. DOI：10.1016/j.jhydrol.2015.09.046.

Schotting RJ, Moser H, Hassanizadeh SM. 1999. High-concentration-gradient dispersion in porous media: Experiments, analysis and approximations. Advances in Water Resources, 22(7): 665−680. DOI：10.1016/S0309-1708(98)00052-9.

Sharma V, Chakma S. 2024. Experimental investigation to check the feasibility of an undersurface barrier for stratified layers to remediate seawater intrusion considering an inclined boundary. Journal of Hydrology, 636: 131283. DOI：10.1016/j.jhydrol.2024.131283.

Shen Y, Xin P, Yu X. 2020. Combined effect of cutoff wall and tides on groundwater flow and salinity distribution in coastal unconfined aquifers. Journal of Hydrology, 581: 124444. DOI：10.1016/j.jhydrol.2019.124444.

Voss C, Provost A. 2010. SUTRA—a Model for saturated–unsaturated, variable density, Groundwater flow with Solute or energy transport. US Geological Survey Water-Resources

Investigations Report, 02-4231.

Voss CI, Souza WR. 1987. Variable density flow and solute transport simulation of regional aquifers containing a narrow freshwater-saltwater transition zone. Water Resource Research, 23(10): 1851−1866. DOI：10.1029/WR023i010p01851.

Walther M, Graf T, Kolditz O, et al. 2017. How significant is the slope of the sea-side boundary for modelling seawater intrusion in coastal aquifers? Journal of Hydrology, 551: 648−659. DOI：10.1016/j.jhydrol.2017.02.031.

Wang F, Li JF, Shi PX, et al. 2019. The impact of sea-level rise on the coast of Tianjin-Hebei, China. China Geology, 2(1): 26−39. DOI：10.31035/cg2018061.

Wang J, Guo Z, Tian Y, et al. 2022. Development and application of sea water intrusion models. Hydrogeology and Engineering Geology, 49(2): 184−194. (in Chinese) DOI：10.16030/j.cnki.issn.1000-3665.202105037.

Watson SJ, Barry DA, Schotting RJ, et al. 2002. Validation of classical density dependent solute transport theory for stable, high-concentration-gradient brine displacements in coarse and medium sands. Advance in Water Resource, 25(6): 611−635. DOI：10.1016/S0309-1708(02)00022-2.

Werner AD, Bakker M, Post VE, et al. 2013. Seawater intrusion processes, investigation, and management: Recent advances and future challenges. Advance in Water Resource, 51: 3−26. DOI：10.1016/j.advwatres.2012.03.004.

Yang X, Cao H, Werner AD, et al. 2024. Experimental and numerical investigation of the effect of air injection on seawater intrusion mitigation. Journal of Hydrology, 642: 131850. DOI：10.1016/j.jhydrol.2024.131850.

Ye Y, Tang T, Xie Y, et al. 2025. Saltwater intrusion in estuarine aquifers through tidal river-groundwater interactions: Three-dimensional experiments and fully-coupled numerical simulations. Journal of Hydrology, 659: 133281. DOI：10.1016/j.jhydrol.2025.133281.

Yu X, He L, Yao R, et al. 2024. Effects of beach nourishment on seawater intrusion in layered heterogeneous aquifers. Journal of Hydrology, 633: 131018. DOI：10.1016/j.jhydrol.2024.131018.

Zhang Q, Volker RE, Lockington DA. 2002. Experimental investigation of contaminant transport in coastal groundwater. Advance in Environment Research, 6(3): 229−237. DOI：10.1016/S1093-0191(01)00054-5.

Zhao S, Su X, Zhang W. 2025. Numerical simulation of thermal effects on seawater intrusion management by coastal cutoff walls. Journal of Environmental Management, 381: 125262. DOI：10.1016/j.jenvman.2025.125262.

Zheng C, Wang PP. 1999. MT3DMS: A modular three-dimensional multispecies transport model for simulation of advection, dispersion, and chemical reactions of contaminants in groundwater systems. Documentation and User's Guide, (No. SERDP991).